

Solution Photophysics, One-Electron Photooxidation, and Photoinitiated Two-Electron Oxidation of Molybdenum(III) Complexes

Abdul K. Mohammed,[†] Ralph A. Isovitsch,[‡] and Andrew W. Maverick*

Department of Chemistry, Louisiana State University, Baton Rouge, Louisiana 70803-1804

Received July 31, 1997

Several six-coordinate Mo(III) complexes phosphoresce and undergo photooxidation in room-temperature solution. The phosphorescence of $(\text{Me}_3[9]\text{aneN}_3)\text{MoX}_3$ ($\text{Me}_3[9]\text{aneN}_3 = 1,4,7\text{-trimethyl-1,4,7-triazacyclononane}$) in $\text{CH}_3\text{-CN}$ at room temperature occurs with the following maxima, lifetimes, and quantum yields: $\text{X} = \text{Cl}$, 1120 nm, 1.0 μs , and 6.1×10^{-5} ; $\text{X} = \text{Br}$, 1130 nm, 0.80 μs , and 9.6×10^{-5} ; and $\text{X} = \text{I}$, 1160 nm, 0.40 μs , and 1.2×10^{-4} , respectively. The phosphorescences are assigned to the $\{^2\text{E}_g, ^2\text{T}_{1g}\} \rightarrow ^4\text{A}_{2g}$ transition. Solutions of $\text{HB}(\text{Me}_2\text{pz})_3\text{Mo}^{\text{III}}\text{Cl}_3 \cdot \text{Me}_2\text{pzH} = 3,5\text{-dimethylpyrazole}$ in CH_3CN , and solid $\text{MoCl}_3(\text{py})_3$ and $(\text{Me}_3[9]\text{aneN}_3)\text{-WCl}_3$, also phosphoresce. $(\text{Me}_3[9]\text{aneN}_3)\text{MoX}_3$ ($\text{X} = \text{Cl, Br, I}$) complexes undergo reversible one-electron photooxidation upon irradiation in the presence of acceptors such as TCNE and chloranil. $(\text{Me}_3[9]\text{aneN}_3)\text{MoX}_3$ ($\text{X} = \text{Br, I}$ only) are photooxidized irreversibly to $[(\text{Me}_3[9]\text{aneN}_3)\text{Mo}^{\text{IV}}\text{X}_3]^+$ by $\text{C}(\text{NO}_2)_4$ in CH_3CN . In $\text{CH}_3\text{-CN-H}_2\text{O}$ (1:1 v/v), photoinitiated two-electron oxidation occurs: the primary photoproduct is Mo(IV), which disproportionates spontaneously to form $[(\text{Me}_3[9]\text{aneN}_3)\text{Mo}^{\text{V}}\text{OX}_2]^+$.

Introduction

We are studying the photochemistry of d^3 complexes of the early transition metals because they are stable in oxidation states with the photophysically attractive d^3 configuration^{1a,2,3} as well as in several adjacent oxidation states. We have applied this stability in multiple oxidation states to the photoinitiated two-electron oxidations of $\text{V}(\text{phen})_3^{2+}$ ^{1b} to VO^{2+} ⁴ and of $\text{Mo}(\text{NCS})_6^{3-}$ to $\text{Mo}_2\text{O}_4(\text{NCS})_6^{4-}$.⁵ Also, we showed that ReCl_6^{2-} undergoes photoinitiated *three-electron* oxidation, producing ReO^{4-} .⁶ Among other Mo(III) complexes, MoCl_6^{3-} appeared well suited for photoredox reactions: its lowest-energy excited state (energy ca. 1.1 eV) has a lifetime of 500 ns.⁷ However, MoCl_6^{3-} is stable only in the presence of extremely high concentrations of Cl^- (e.g. in concentrated $\text{HCl}(\text{aq})$). In the present work, we have examined the solution photophysics and photoredox reactions of several molybdenum(III) complexes that are stable in more conventional solvents. The most promising species, because of their well-defined absorption and emission spectra and their facile photoredox reactions, contain the 1,4,7-trimethyl-1,4,7-triazacyclononane, or $\text{Me}_3[9]\text{aneN}_3$, ligand; they were first reported by Wieghardt and co-workers.^{8,9} (Enemark

and co-workers have recently compared these complexes with those of tris(3,5-dimethylpyrazolyl)methane.¹⁰ We find that one-electron photooxidation, followed by disproportionation, is a facile route for photoinitiated two-electron oxidation in several systems. We expect that these net two-electron transformations will prove to be a common feature in the photochemistry of second- and third-row metal complexes.

Experimental Section

Materials. Chloranil (MCB) was purified by recrystallization from 1,2-dichloroethane. Tetracyanoethylene (TCNE; Aldrich) was purified by recrystallization from chlorobenzene and subsequent sublimation. Benzylviologen dichloride (Sigma Chemical Co.) was converted to the tetrafluoroborate salt by the general method of Hunig and co-workers,¹¹ and this was purified by recrystallization from aqueous ethanol. $\text{MoCl}_3(\text{py})_3$ was prepared from K_3MoCl_6 (Sharpe Chemical Co., Burbank CA) by the method of Jonassen and Bailin.¹² The method of Trofimenko¹³ was used for preparing $\text{KHB}(\text{Me}_2\text{pz})_3 \cdot (\text{Et}_4\text{N})[\text{HB}(\text{Me}_2\text{pz})_3\text{Mo}^{\text{III}}\text{Cl}_3]$ was prepared using the procedure of Millar and co-workers,¹⁴ modified by adding small amounts of water to facilitate the precipitation of the product following ethanol reduction of $\text{HB}(\text{Me}_2\text{pz})_3\text{Mo}^{\text{IV}}\text{Cl}_3$. Other materials and solvents were of the highest grade commercially available and were used as received. Samples for photochemical measurements were prepared by using drybox, Schlenk or high-vacuum techniques.

$\text{Me}_3[9]\text{aneN}_3$ and Its Mo and W Complexes. This ligand has been prepared by a variety of methods;¹⁵ we outline here the procedure that we found to be most convenient. Diethylenetriamine was tosylated,¹⁶

[†] Present address: Department of Chemistry, North Carolina A&T State University, Greensboro, NC 27411.

[‡] Present address: Division of Science and Mathematics, University of the Virgin Islands, St. Thomas, VI 00802.

- (1) (a) Furlani, C. *Coord. Chem. Rev.* **1966**, *1*, 51–57. (b) Abbreviations: bpy, 2,2'-bipyridine; bpyz, 2,2'-bipyrazine; BV^{2+} , benzylviologen (1,1'-bis(phenylmethyl)-4,4'-bipyridinium); chloranil, 2,3,5,6-tetrachloro-1,4-benzoquinone; $\text{HB}(\text{Me}_2\text{pz})_3^-$, hydrotris(3,5-dimethyl-1-pyrazolyl)borate; $\text{Me}_3[9]\text{aneN}_3$, 1,4,7-trimethyl-1,4,7-triazacyclononane; phen, 1,10-phenanthroline; py, pyridine; TCNE, tetracyanoethylene (ethenetetracarboxynitrile).
- (2) Fleischauer, P. D.; Fleischauer, P. *Chem. Rev.* **1970**, *70*, 199–230.
- (3) Hoffman, M. Z.; Serpone, N.; Jamieson, M. A. *Coord. Chem. Rev.* **1981**, *39*, 121–179.
- (4) Shah, S. S.; Maverick, A. W. *Inorg. Chem.* **1987**, *26*, 1559–1562.
- (5) Yao, Q.; Maverick, A. W. *J. Am. Chem. Soc.* **1986**, *108*, 5364–5365.
- (6) Maverick, A. W.; Lord, M. D.; Yao, Q.; Henderson, L. J., Jr. *Inorg. Chem.* **1991**, *30*, 553–558.
- (7) Yao, Q.; Maverick, A. W. *Inorg. Chem.* **1988**, *27*, 1669–1670.

- (8) Backes-Dahmann, G.; Herrmann, W.; Wieghardt, K.; Weiss, J. *Inorg. Chem.* **1985**, *24*, 485–491.
- (9) Backes-Dahmann, G.; Wieghardt, K. *Inorg. Chem.* **1985**, *24*, 4049–4054.
- (10) Dhawan, I. K.; Bruck, M. A.; Schilling, B.; Grittini, C.; Enemark, J. H. *Inorg. Chem.* **1995**, *34*, 3801–3808.
- (11) Hünig, S.; Gross, J.; Lier, E. F.; Quast, H. *Justus Liebigs Ann. Chem.* **1973**, 339–358.
- (12) Jonassen, H. B.; Bailin, L. J. *Inorg. Synth.* **1963**, *7*, 140–142.
- (13) Trofimenko, S. *J. Am. Chem. Soc.* **1967**, *89*, 6288–6294.
- (14) Millar, M.; Lincoln, S.; Koch, S. A. *J. Am. Chem. Soc.* **1982**, *104*, 288–289.

and the conjugate base of the resulting tritosyl compound treated with ethylene glycol ditosylate to produce 1,4,7-tritosyl-1,4,7-triazacyclononane ($\text{Ts}_3[9]\text{aneN}_3$), which was converted to $[9]\text{aneN}_3 \cdot 3\text{HBr}$ by treatment with concentrated $\text{HBr}(\text{aq})$.¹⁷ A suspension of $[9]\text{aneN}_3 \cdot 3\text{HBr}$ in benzene was treated with excess $\text{NaOH}(\text{s})$, with stirring, over a period of 48 h. Solid NaBr and NaOH were filtered off, and the filtrate was evaporated to produce crude 1,4,7-triazacyclononane, $[9]\text{-aneN}_3$, as a nearly colorless oil. Pure $[9]\text{aneN}_3$ is a low-melting solid; however, the oil was pure enough, as judged by $^1\text{H NMR}$, for methylation.¹⁸ Methylation with $\text{HCHO}(\text{aq})$ and 98% HCO_2H ¹⁹ was followed by treatment with excess $\text{NaOH}(\text{aq})$ and extraction with benzene. The benzene layer was dried over Na_2SO_4 and evaporated, giving $\text{Me}_3[9]\text{aneN}_3$ as a pale yellow oil which was essentially pure by $^1\text{H NMR}$.

($\text{Me}_3[9]\text{aneN}_3$) MoX_3 ($X = \text{Cl, Br, I}$)⁸ and ($\text{Me}_3[9]\text{aneN}_3$) WCl_3 ⁹ were prepared by literature methods. These were characterized by electronic and IR spectroscopy and by cyclic voltammetry where appropriate. All of these measurements, except for a few of the bands observed in our electronic spectra, agreed with those reported by Wieghardt and co-workers. Where there were discrepancies in the electronic spectra, we repeated the preparations and found that our data were reproducible; the purity of all such samples was also checked by microanalysis (Desert Analytics, Tucson, AZ).

Instruments and Procedures. Cyclic voltammograms were recorded by using either a PAR model 174A Polarographic Analyzer or a Wenking TS70/1 potentiostat with a home-built microcomputer interface. The cell contained Pt working and counter electrodes and an aqueous Ag/AgCl (3 M NaCl) reference electrode. The half-wave potential for the Fc/Fc^+ ($\text{Fc} = \text{ferrocene}$) reference redox couple in CH_3CN under these conditions was 0.47 V.

Electronic absorption spectra were recorded on an Aviv 14DS spectrophotometer. Luminescence measurements were performed in the front-face mode using a Hamamatsu R406 PMT or a Ge photodiode, with a modified Spex fluorometer, and the spectra were corrected for variations in detection efficiency with wavelength, as previously described.⁶ The phosphorescence spectra in Figures 1–3 were all recorded with a bandpass of ca. 15 nm.

Emission quantum yields were measured in deoxygenated solutions (CH_3CN , 25 °C, 436 nm excitation, 15 min N_2 bubbling) by comparison with $[\text{Ru}^{\text{II}}(\text{bpy})_2(\text{bpyz})]^{2+}$ ($\lambda_{\text{max,em}} = 710 \text{ nm}$; $\Phi_{\text{em}} 0.019$ in propylene carbonate at room temperature²⁰). Absorbances for the Ru^{II} standard and the Mo^{III} sample were between 0.06 and 0.14; they were matched within 5% in any one experiment. The spectra were corrected for detector response, differences in refractive indices, and reabsorption of emitted light due to vibrational overtones in the near-IR.^{21–23} They are plotted (in Figures 1–3) in units proportional to quanta per nm bandwidth.

Experiments on the nanosecond timescale utilized excimer (XeCl , 308 nm) or $\text{Nd}:\text{YAG}$ lasers (532 and 355 nm). Kinetic data from these experiments were recorded and analyzed by using Hewlett-Packard or Biomation/Tektronix digitizer/microcomputer systems. Near-infrared

(15) Chaudhuri, P.; Wieghardt, K. *Prog. Inorg. Chem.* **1987**, *35*, 329–436.

(16) Koyama, H.; Yoshino, T. *Bull. Chem. Soc. Jpn.* **1972**, *45*, 481–484.

(17) Wieghardt, K.; Schmidt, W.; Nuber, B.; Weiss, J. *Chem. Ber.* **1979**, *112*, 2220–2230.

(18) White, D. W.; Karcher, R. A.; Verkade, J. G. *J. Am. Chem. Soc.* **1979**, *101*, 4921–4925.

(19) (a) Wieghardt, K.; Chaudhuri, P.; Nuber, B.; Weiss, J. *Inorg. Chem.* **1982**, *21*, 3086–3090. (b) This procedure is similar to those used for methylation of cyclam and related macrocycles (Barefield, E. K.; Wagner, F. *Inorg. Chem.* **1973**, *12*, 2435–2439; Buxtorf, R.; Kaden, T. A. *Helv. Chim. Acta* **1974**, *57*, 1035–1042). We found that adding a small amount of H_2O to the $\text{HCO}_2\text{H}/\text{HCHO}(\text{aq})$ methylation mixture, as suggested by some authors, made little difference. It was not necessary to isolate $\text{Me}_3[9]\text{aneN}_3 \cdot 3\text{HCl}$ from the methylation mixture; instead, it was converted directly to $\text{Me}_3[9]\text{aneN}_3$.

(20) Rillema, D. P.; Allen, G.; Meyer, T. J.; Conrad, D. *Inorg. Chem.* **1983**, *22*, 1617–1622.

(21) Demas, J. N.; Crosby, G. A. *J. Phys. Chem.* **1971**, *75*, 991–1024.

(22) Demas, J. N. *Excited-State Lifetime Measurements*; Academic: New York, 1983; pp 149–153.

(23) Parker, C. A.; Rees, W. T. *Analyst* **1960**, *85*, 587–600.

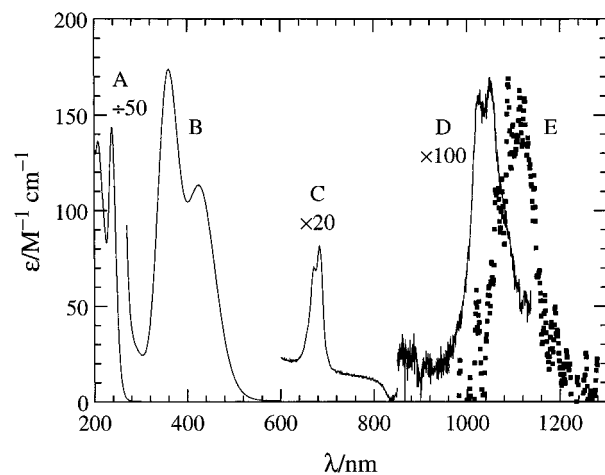


Figure 1. Electronic absorption (—) and corrected emission (■) spectra for ($\text{Me}_3[9]\text{aneN}_3$) MoCl_3 in CH_3CN at room temperature. The emission spectrum was recorded using a degassed 4×10^{-3} M solution, with 355-nm excitation. Assignments: A, LMCT; B, $^4\text{A}_{2g} \rightarrow ^4\text{T}_{2g}, ^4\text{T}_{1g}$; C, $^4\text{A}_{2g} \rightarrow ^2\text{T}_{2g}$; D, $^4\text{A}_{2g} \rightarrow \{^2\text{T}_{1g}, ^2\text{E}_g\}$; E, phosphorescence ($\{^2\text{T}_{1g}, ^2\text{E}_g\} \rightarrow ^4\text{A}_{2g}$).

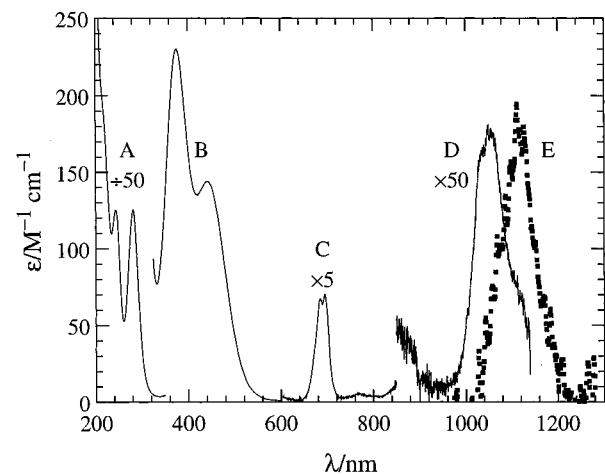


Figure 2. Electronic absorption (—) and corrected emission (■) spectra for ($\text{Me}_3[9]\text{aneN}_3$) MoBr_3 in CH_3CN at room temperature. The emission spectrum was recorded using a degassed 1×10^{-3} M solution, with 370-nm excitation. Assignments: A, LMCT; B, $^4\text{A}_{2g} \rightarrow ^4\text{T}_{2g}, ^4\text{T}_{1g}$; C, $^4\text{A}_{2g} \rightarrow ^2\text{T}_{2g}$; D, $^4\text{A}_{2g} \rightarrow \{^2\text{T}_{1g}, ^2\text{E}_g\}$; E, phosphorescence ($\{^2\text{T}_{1g}, ^2\text{E}_g\} \rightarrow ^4\text{A}_{2g}$).

luminescence lifetimes were measured with the same apparatus, but using a Ge photodiode (Judson 2 mm diameter) operated at room temperature (3 V reverse bias; response time ca. 50 ns). The experimental detector response function was used to estimate actual emission lifetimes by deconvolution.²² These lifetimes, and the emission quantum yields and electron-transfer quenching rate constants, were reproducible within $\pm 10\%$.

Continuous photolyses with irreversible electron acceptors were performed by using appropriate cutoff filters to ensure that only the Mo complexes were irradiated. The quantum yield for the photooxidation of ($\text{Me}_3[9]\text{aneN}_3$) $\text{Mo}^{\text{III}}\text{Br}_3$ to $[(\text{Me}_3[9]\text{aneN}_3)\text{Mo}^{\text{IV}}\text{Br}_3]^+$ by $\text{C}(\text{NO}_2)_4$ was determined by using a single 532 nm pulse (360 mJ) from a $\text{Nd}:\text{YAG}$ laser as the excitation source. The single pulse was required because the products, $\text{C}(\text{NO}_2)_3^-$ and $[(\text{Me}_3[9]\text{aneN}_3)\text{Mo}^{\text{IV}}\text{Br}_3]^+$, absorb more strongly than the reactants at nearly all wavelengths.

Results

Electronic Absorption Spectra. The absorption spectra of MoCl_6^{3-} and $\text{Mo}(\text{NCS})_6^{3-}$ have been discussed previously.^{5,7,24–26}

(24) Jørgensen, C. K. *Adv. Chem. Phys.* **1963**, *5*, 33–146.

Table 1. Electronic Absorption Spectra of Mo^{III} and W^{III} Complexes^a

complex	solvent	LMCT	$^4A_{2g} \rightarrow ^4T_{1g}, ^4T_{2g}$	$^4A_{2g} \rightarrow ^2T_{2g}$	$^4A_{2g} \rightarrow \{^2E_g, ^2T_{1g}\}$
MoCl ₆ ³⁻ ^b	concd HCl	<300	420 (40), 520 (30)	670 (1.4)	1050 (0.5)
(Me ₃ [9]aneN ₃)MoCl ₃	CH ₃ CN	208, 238	360 (170), 425 (110)	672 (2.8), 684 (3.2)	1050 (1.3)
(Me ₃ [9]aneN ₃)MoBr ₃	CH ₃ CN	215 sh, 244, 282	376 (230), 442 (140)	685 (13), 695 (14)	1055 (3.3)
(Me ₃ [9]aneN ₃)MoI ₃	CH ₃ CN	260 sh, 305, 334, 374	470 sh ^c	722 (80)	1083 (10)
MoCl ₃ (py) ₃ ^d	pyridine	<500	<i>e</i>	690	1140
HB(Me ₂ pz) ₃ MoCl ₃ ⁻	CH ₃ CN	<500	<i>e</i>	690	1250
(Me ₃ [9]aneN ₃)WCl ₃ ^f	CH ₃ CN	310	480 br	650–720	1050–1300

^a λ_{\max}/nm ; $\epsilon/M^{-1} \text{ cm}^{-1}$ in parentheses; sh = shoulder; br = broad. ^b Data from ref 7. ^c $^4A_{2g} \rightarrow ^4T_{2g}$; $^4A_{2g} \rightarrow ^4T_{1g}$ is buried under charge-transfer transitions. ^d Data from refs 25, 28, and 29. ^e The spin-allowed d–d transitions are buried under charge-transfer transitions. ^f The low solubility of this complex made detailed study of its absorption spectrum difficult.

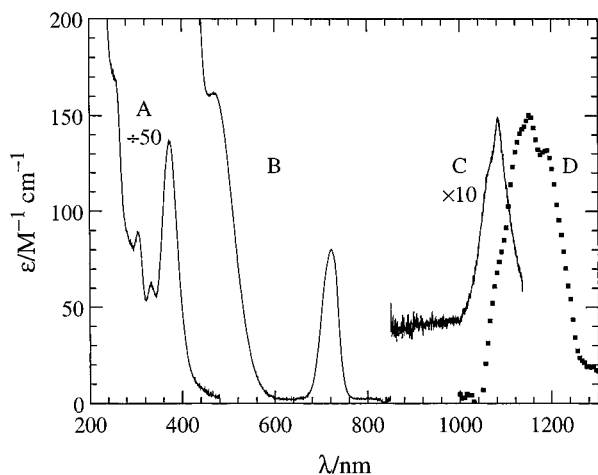


Figure 3. Electronic absorption (—) and corrected emission (■) spectra for (Me₃[9]aneN₃)MoI₃ in CH₃CN at room temperature. The emission spectrum was recorded using a degassed 2×10^{-3} M solution, with 436-nm excitation. Assignments: A, LMCT; B, $^4A_{2g} \rightarrow ^4T_{2g}$ (470 nm); $^4A_{2g} \rightarrow ^4T_{2g}$ obscured by LMCT and $^4A_{2g} \rightarrow ^2T_{2g}$ (722 nm); C, $^4A_{2g} \rightarrow \{^2T_{1g}, ^2E_g\}$; D, phosphorescence ($\{^2T_{1g}, ^2E_g\} \rightarrow ^4A_{2g}$).

Among the other complexes we have studied, (Me₃[9]aneN₃)MoX₃ (X = Cl, Br, I) show the best-defined spectra; see Figures 1–3 and data in Table 1. These are very similar to those reported for MoCl₆³⁻.^{7,27} We assign the weak bands in the 660–750 and 1000–1150 nm regions in the complexes to the spin-forbidden transitions $^4A_{2g} \rightarrow ^2T_{2g}$ and $^4A_{2g} \rightarrow \{^2E_g, ^2T_{1g}\}$ respectively. The absorption bands in the 350–500 nm range are due to the spin-allowed d–d transitions $^4A_{2g} \rightarrow ^4T_{2g}$ and $^4A_{2g} \rightarrow ^4T_{1g}$, the latter appearing at higher energy. Intense bands at higher energy are attributable to ligand-to-metal charge transfer (LMCT), at increasing energy in the order I < Br < Cl, as expected. In (Me₃[9]aneN₃)MoI₃, the first LMCT band, at 374 nm, obscures the second spin-allowed d–d transition ($^4A_{2g} \rightarrow ^4T_{1g}$).

The spectra of HB(Me₂pz)₃Mo^{III}Cl₃⁻¹⁴ and MoCl₃(py)₃^{25,28,29} show spin-forbidden absorption bands, $^4A_{2g} \rightarrow ^2T_{2g}$ and $^4A_{2g} \rightarrow \{^2E_g, ^2T_{1g}\}$, with peaks near those found for the other Mo^{III} complexes; see Table 1. In both cases, the spin-allowed d–d bands are obscured by intense charge-transfer transitions beginning near 500 nm.

Solutions of (Me₃[9]aneN₃)WCl₃ in CH₃CN show a number of weak, narrow absorption bands in the 650–720 and 1050–

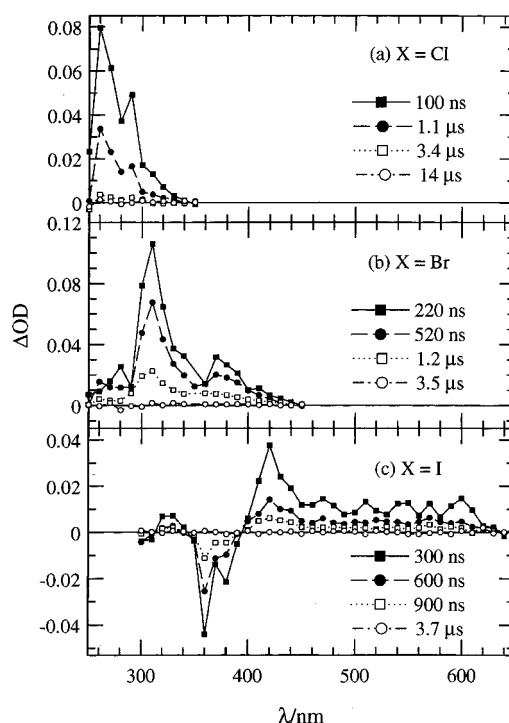


Figure 4. Transient difference spectra for (Me₃[9]aneN₃)MoX₃ (X = Cl, Br, I) in CH₃CN at room temperature. The spectra were recorded at the indicated delay times following 10-ns flashes at 355 nm.

1300 nm regions. These features are similar to those previously reported for ReCl₆²⁻.^{6,7,30} Thus, in analogy with ReCl₆²⁻, we assign these bands to the $^4A_{2g} \rightarrow ^2T_{2g}$ and $^4A_{2g} \rightarrow \{^2E_g, ^2T_{1g}\}$ transitions respectively; the two ²T terms are expected to be split substantially by spin–orbit coupling.

Transient Absorption Spectra. Pulsed-laser irradiation (10 ns, 355 nm) of the three (Me₃[9]aneN₃)MoX₃ complexes in CH₃CN solution produces transient absorption signals (as well as bleaching for X = I); these are illustrated in Figure 4. All of these signals decay exponentially, with lifetimes similar to those observed in emission (see Table 2). The transient absorption signals are most intense at relatively high energy. Also, like the intense bands in the ground-state absorption spectra, the major excited-state features occur at increasing energy in the order I < Br < Cl. Therefore, they are probably associated with excited-state LMCT transitions. With (Me₃[9]aneN₃)MoI₃, bleaching of the intense ground-state LMCT absorption band at 370 nm is also observed; this decays with a lifetime similar to those observed in emission and transient absorption. The bleaching and absorption signals for (Me₃[9]aneN₃)MoI₃ are

(25) König, E.; Schäfer, H. J. *Z. Phys. Chem. N. F.* **1960**, *26*, 371–403.

(26) (a) Pruchnik, F.; Wajda, S. *Rocz. Chem.* **1969**, *43*, 1379–1386. (b) Schmidtke, H.-H. *Ber. Bunsen-Ges. Phys. Chem.* **1967**, *71*, 1138–1145.

(27) Flint, C. D.; Paulusz, A. G. *Mol. Phys.* **1981**, *44*, 925–938.

(28) Komorita, T.; Miki, S.; Yamada, S. *Bull. Chem. Soc. Jpn.* **1965**, *38*, 123–129.

(29) Furlani, C.; Piovesana, O. *Mol. Phys.* **1965**, *9*, 341–347.

(30) (a) Eisenstein, J. C. *J. Chem. Phys.* **1961**, *34*, 1628–1648. (b) Black, A. M.; Flint, C. D. *J. Chem. Soc., Faraday Trans. 2* **1977**, *73*, 877–885. (c) Flint, C. D.; Paulusz, A. G. *Mol. Phys.* **1981**, *43*, 321–334.

Table 2. Room-Temperature Phosphorescence and Redox Properties of Mo^{III} and W^{III} Complexes

complex	medium	$\lambda_{\max}/\text{nm}^a$	$\tau_{\text{abs}}/\mu\text{s}^{b,c}$	$\tau_{\text{em}}/\mu\text{s}^{b,c}$	$\Phi^{c,d}$	$E(^{+2}E_g^{\text{II}})/\text{cm}^{-1}^e$	$E_{1/2}/\text{V}^f$	$E^*_{1/2}/\text{V}^f$
MoCl ₆ ³⁻	concd HCl	1095 ^h	0.55 ^g	0.48 ^g		9239 ⁱ	-0.76 ^j	-1.92
(Me ₃ [9]aneN ₃)MoCl ₃	CH ₃ CN	1120	1.05	0.96	6.1×10^{-5}	9200	0.39 ^k	-0.75
(Me ₃ [9]aneN ₃)MoBr ₃	CH ₃ CN	1130	0.75	0.80	9.6×10^{-5}	9200	0.50 ^k	-0.64
(Me ₃ [9]aneN ₃)MoI ₃	CH ₃ CN	1160	0.35	0.45	1.2×10^{-4}	8900	0.53 ^k	-0.58
MoCl ₃ (py) ₃	solid	1400 ^h				ca. 8000		
HB(Me ₂ Pz) ₃ MoCl ₃ ⁻	CH ₃ CN	> 1250 ^{h,l}				< 8000	0.02	> -0.98
(Me ₃ [9]aneN ₃)WCl ₃	solid	1400 ^h				ca. 7400	-0.39	-1.3

^a Corrected, unless otherwise noted. ^b Lifetimes measured in transient absorption (τ_{abs}) and in emission (τ_{em}). ^c $\pm 10\%$. ^d Quantum yield in dilute solution; 436-nm excitation. ^e Estimated by averaging absorption and emission maxima. ^f Half-wave potentials (Mo(III)/Mo(IV)) vs Fc/Fc⁺ in CH₃CN: $E_{1/2}$, ground-state; $E^*_{1/2}$, excited-state (estimated as $E_{1/2} - E(^{+2}E_g^{\text{II}})$ (in eV)). ^g Reference 7. ^h Uncorrected. ⁱ Spectroscopic 0–0 energy, from ref 27. ^j In CH₂Cl₂: Heath, G. A.; Moock, K. A.; Sharp, D. W. A.; Yellowlees, L. J. *J. Chem. Soc., Chem. Commun.* **1985**, 1503–1505. ^k Reference 8. ^l Phosphorescence too weak for reliable estimate of λ_{\max} .

approximately equal in magnitude; thus, we estimate that the excited-state absorption band has ϵ_{\max} ca. 7000 M⁻¹ cm⁻¹.

Emission Spectra. Like MoCl₆³⁻ and Mo(NCS)₆³⁻,⁷ many of the d³ complexes studied herein luminesce in solution at room temperature. The corrected phosphorescence maxima of the (Me₃[9]aneN₃)MoX₃ complexes in acetonitrile are in the 1120–1160 nm range. The excited-state lifetimes for dilute CH₃CN solutions of (Me₃[9]aneN₃)MoX₃, estimated by averaging the values obtained in transient absorption and emission, are 1.0 (X = Cl), 0.80 (X = Br), and 0.40 μs (X = I). The measured lifetime of a saturated solution of (Me₃[9]aneN₃)MoCl₃, ca. 4 mM, was approximately 20% shorter. Phosphorescence quantum yields (see Table 2) are largest for the iodide complex.

HB(Me₂pz)₃MoCl₃⁻ shows weak phosphorescence, with a peak near 1300 nm in CH₃CN solution at room temperature. *mer*-MoCl₃(py)₃ phosphoresces only in the solid state, at ca. 1400 nm. The tungsten(III) complex (Me₃[9]aneN₃)WCl₃ also phosphoresces: emission occurs near 1400 nm in the solid state at room temperature. As far as we are aware, this is the first example of luminescence from any tungsten(III) complex.

We found that solutions of these last three complexes, HB(Me₂pz)₃Mo^{III}Cl₃⁻, MoCl₃(py)₃, and (Me₃[9]aneN₃)W^{III}Cl₃, were not sufficiently stable for photochemical study. The tungsten(III) complex has also been reported to be more difficult to purify and less stable than the analogous Mo(III) species.^{9,31} Therefore, in our photochemical experiments, we concentrated on the three (Me₃[9]aneN₃)MoX₃ complexes.

Reversible One-Electron Photooxidation. Wieghardt and co-workers showed that (Me₃[9]aneN₃)Mo^{III}X₃ can undergo chemical and electrochemical outer-sphere one-electron oxidation to [(Me₃[9]aneN₃)Mo^{IV}X₃]⁺ and further oxidation to [(Me₃[9]aneN₃)Mo^VOX₂]⁺ and [(Me₃[9]aneN₃)Mo^{VI}O₂X]⁺.⁸ We wished to determine whether these reactions could be carried out photochemically.

The phosphorescences of the (Me₃[9]aneN₃)Mo^{III}X₃ complexes are quenched by strong electron acceptors such as TCNE, chloranil, and benzylviologen. We attribute this quenching to reversible photochemical electron transfer from Mo^{III} to the electron acceptors. Relatively strong acceptors ($E_{1/2}$: TCNE^{0/-}, -0.16 V;⁵ chloranil^{0/-}, -0.36 V;⁶ BV^{2+/+}, -0.76 V³² vs Fc/Fc⁺ in CH₃CN) are required for efficient quenching because the complexes are difficult to oxidize: see redox potentials in Table 2. Rate constants derived from Stern–Volmer analysis of the quenching data are collected in Table 3.

2,3-Dichloro-5,6-dicyano-1,4-benzoquinone (DDQ), another powerful acceptor, could not be used in these experiments because it formed strongly absorbing donor–acceptor charge-

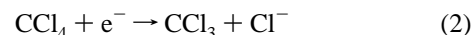
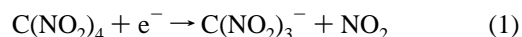
Table 3. Quenching Rate Constants/M⁻¹ s⁻¹ from Phosphorescence Quenching^a

complex	electron acceptor		
	TCNE	chloranil	BV ²⁺
(Me ₃ [9]aneN ₃)MoCl ₃	5.2×10^9	4.0×10^9	8.4×10^8
(Me ₃ [9]aneN ₃)MoBr ₃	4.6×10^9	3.8×10^9	2.4×10^8
(Me ₃ [9]aneN ₃)MoI ₃	5.3×10^9	3.8×10^9	$< 1 \times 10^7$ ^b

^a In CH₃CN, at room temperature; values were reproducible within $\pm 10\%$. ^b Quenching not observed. Value given is estimated upper limit; see text for discussion.

transfer complexes with (Me₃[9]aneN₃)MoX₃. Also, the phosphorescence of (Me₃[9]aneN₃)Mo^{III}I₃ was not quenched measurably by benzylviologen. Thus, the value given in Table 3 is an upper limit, based on the measured lifetime of (Me₃[9]aneN₃)Mo^{III}I₃ and the maximum available concentration of benzylviologen (ca. 0.05 M).

Irreversible Photooxidation. We also studied the permanent photooxidation of (Me₃[9]aneN₃)MoX₃ by tetranitromethane (C(NO₂)₄) and carbon tetrachloride (CCl₄). These are known to function as irreversible electron acceptors:^{33,34}



Irradiation ($\lambda > 420$ nm) of (Me₃[9]aneN₃)Mo^{III}Br₃ in the presence of C(NO₂)₄ in CH₃CN causes a color change from yellow to red within a few minutes. Figure 5 shows increases in the absorbances due to C(NO₂)₃⁻ (350 nm) and [(Me₃[9]aneN₃)Mo^{IV}Br₃]⁺ (490 nm) during photolysis.

We could not measure the quantum yield for this reaction by a simple continuous photolysis experiment, because the Mo(IV) product absorbs more strongly than the Mo(III) starting material at all reasonable irradiation wavelengths. Instead, we estimated the quantum yield by using a single 532-nm pulse (360 mJ) from a frequency-doubled Nd:YAG laser: this pulse is sufficiently short (ca. 10 ns) that the amount of photooxidation during the pulse is expected to be negligible. On the basis of the results of this experiment (2 mM Mo^{III}; 3 mM C(NO₂)₄ in CH₃CN), the quantum yield for formation of [(Me₃[9]aneN₃)Mo^{IV}Br₃]⁺ is ca. 0.06.

(Me₃[9]aneN₃)Mo^{III}Br₃ is also photooxidized by C(NO₂)₄ in a 1:1 (v/v) CH₃CN–H₂O solution. In this case the oxidized product obtained was [(Me₃[9]aneN₃)Mo^VOBr₂]⁺, as judged by

- (33) See, for example: (a) Masnovi, J. M.; Kochi, J. K. *J. Am. Chem. Soc.* **1985**, *107*, 7880–7893. (b) Masnovi, J. M.; Kochi, J. K.; Hilinski, E. F.; Rentzepis, P. M. *J. Am. Chem. Soc.* **1986**, *108*, 1126–1135. (34) Engel, P. S.; Keys, D. E.; Kitamura, A. *J. Am. Chem. Soc.* **1985**, *107*, 4964–4975 and references therein.

(31) Wieghardt, K.; Backes, G. Personal communication.

(32) Mohammed, A. K.; Fronczek, F. R.; Maverick, A. W. *Inorg. Chim. Acta* **1994**, *226*, 25–31.

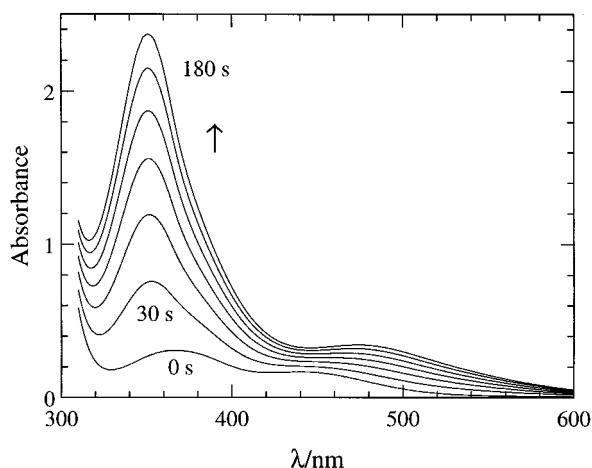


Figure 5. Electronic absorption spectral changes accompanying the photolysis ($\lambda > 420$ nm) at room temperature of ca. 1×10^{-3} M $(\text{Me}_3[9]\text{aneN}_3)\text{MoBr}_3$ and ca. 1.5×10^{-3} M $\text{C}(\text{NO}_2)_4$ in CH_3CN . Spectra were recorded before photolysis ("0 s") and then at 30-s intervals, showing gradually increasing absorbance at all wavelengths corresponding to generation of $(\text{Me}_3[9]\text{aneN}_3)\text{Mo}^{\text{IV}}\text{Br}_3^+$.

its IR (ν_{MoO}) and electronic absorption spectra.⁸ No reaction was observed in the dark for either of these mixtures.

$(\text{Me}_3[9]\text{aneN}_3)\text{MoI}_3$ undergoes similar irreversible photooxidation with $\text{C}(\text{NO}_2)_4$. Irradiation of a solution of $(\text{Me}_3[9]\text{aneN}_3)\text{MoI}_3$ and $\text{C}(\text{NO}_2)_4$ in dry CH_3CN leads to a change in color from orange to green. The band at 720 nm ($\text{Mo}^{\text{III}}, {}^4\text{A}_{2g} \rightarrow {}^2\text{T}_{2g}$) disappears, while a more intense band grows in near 600 nm. We assign the new 600-nm band in the green irradiated solutions to a LMCT transition in $[(\text{Me}_3[9]\text{aneN}_3)\text{Mo}^{\text{IV}}\text{I}_3]^+$, because of its intensity (ϵ at least $5000 \text{ M}^{-1} \text{ cm}^{-1}$, on the basis of the ratio of absorbance changes at 600 and 720 nm) and its lower energy relative to the first LMCT band in $[(\text{Me}_3[9]\text{aneN}_3)\text{Mo}^{\text{IV}}\text{Br}_3]^+$. When the photooxidation is carried out in a $\text{CH}_3\text{CN}-\text{H}_2\text{O}$ mixture, $[(\text{Me}_3[9]\text{aneN}_3)\text{Mo}^{\text{V}}\text{OI}_2]^+$ is formed. Compared to the experiments with $(\text{Me}_3[9]\text{aneN}_3)\text{Mo}^{\text{III}}\text{Br}_3$ described above, photooxidations of the iodide complex are less clean. Substantial amounts of other absorbing products are formed, which we were unable to identify.

We also attempted to use $\text{C}(\text{NO}_2)_4$ as an irreversible electron acceptor for photooxidation of $(\text{Me}_3[9]\text{aneN}_3)\text{MoCl}_3$. However, permanent reaction occurs in this case even in the dark, leading to new bands (a shoulder near 400 nm and a second band at 850 nm, in addition to the expected peak at 350 nm due to $\text{C}(\text{NO}_2)_3^-$). Similar changes occur in mixtures of $(\text{Me}_3[9]\text{aneN}_3)\text{MoCl}_3$ and CCl_4 in CH_3CN solution (although this oxidation by CCl_4 is accelerated by irradiation). No changes occurred when solutions of $(\text{Me}_3[9]\text{aneN}_3)\text{Mo}^{\text{III}}\text{X}_3$ ($\text{X} = \text{Br}, \text{I}$) were irradiated in the presence of CCl_4 .

We also performed cyclic voltammetry experiments in CH_3CN with and without added H_2O . Solutions in dry CH_3CN showed quasireversible one-electron oxidation, as previously reported by Wiegardt et al.⁸ Addition of varying amounts of water to these solutions appeared to make the oxidation wave less reversible, but we could not measure the changes easily because of a larger new irreversible oxidation wave attributable to water oxidation at slightly more positive potentials (ca. 1 V vs Fc/Fc^+). Addition of aqueous acid (0.1 M H_2SO_4) instead of pure water was more successful: the water oxidation wave was shifted in the positive direction, so that the $\text{Mo}(\text{III})/\text{Mo}(\text{IV})$ wave was better resolved. For both $(\text{Me}_3[9]\text{aneN}_3)\text{Mo}^{\text{III}}\text{Br}_3$ and $(\text{Me}_3[9]\text{aneN}_3)\text{Mo}^{\text{III}}\text{I}_3$, addition of increasing amounts

Table 4. Peak Current Ratios $i_{\text{pc}}/i_{\text{pa}}$ for $(\text{Me}_3[9]\text{aneN}_3)\text{MoX}_3^{0/+}$ from Cyclic Voltammetry^a

X = Br		X = I	
V/mL	$i_{\text{pc}}/i_{\text{pa}}$	V/mL	$i_{\text{pc}}/i_{\text{pa}}$
0	0.93	0	0.80
1.0	0.88	0.1	0.79
2.0	0.81	0.2	0.76
3.0	0.75	0.3	0.53
4.0	0.69	0.4	0.52
5.0	0.62	0.5	0.47

^a The indicated volume of 0.1 M H_2SO_4 was added to 7.0 mL of CH_3CN (0.1 M $\text{Bu}_4\text{NO}_3\text{SCF}_3$) containing 1.0 mM $\text{Mo}(\text{III})$ complex. Scan rate 100 mV s^{-1} ; Pt electrode.

of $\text{H}_2\text{SO}_4(\text{aq})$ caused the ratio of return (cathodic) current to oxidation current ($i_{\text{pc}}/i_{\text{pa}}$) for the $\text{Mo}(\text{III})/\text{Mo}(\text{IV})$ wave to decrease (see data in Table 4). This effect was more pronounced at slower scan rates. These results are as expected if oxidation of $(\text{Me}_3[9]\text{aneN}_3)\text{Mo}^{\text{III}}\text{X}_3$ in an aqueous medium is followed by reaction of electrogenerated $(\text{Me}_3[9]\text{aneN}_3)\text{Mo}^{\text{IV}}\text{X}_3^+$ with H_2O .

Discussion

Electronic Spectra of Second-Row d^3 Complexes. The species studied here differ in two ways from those of first-row $3d^3$ ions. First, the ligand-field strengths (represented by $10Dq$) for these complexes are much larger, causing the spin-allowed $d-d$ transitions to be at higher energies for the same ligand environment. Second, interelectronic repulsion (represented by the Racah parameter B) is considerably weaker than in first-row species. The energies of the lowest-lying doublet terms, ${}^2\text{E}_g$, ${}^2\text{T}_{1g}$, and ${}^2\text{T}_{2g}$, all of which arise from the same strong-field electronic configuration (t_{2g}^3) as the ground ${}^4\text{A}_{2g}$ term, depend primarily on B .³⁵ Thus, they are lower in energy than with first-row d^3 metals. The major difference between second- and third-row complexes (as seen, for example, in ReCl_6^{2-} and $(\text{Me}_3[9]\text{aneN}_3)\text{W}^{\text{III}}\text{Cl}_3$) is the significant increase in spin-orbit coupling, which leads to larger splittings of the excited ${}^2\text{T}_{1g}$ and ${}^2\text{T}_{2g}$ terms.

Photophysics. Many of the absorption spectral features of the $\text{Me}_3[9]\text{aneN}_3$ complexes (see Table 2) were originally reported by Wiegardt and co-workers.^{8,9} Most of the new data in Table 2 deal with the lowest-energy $\{{}^2\text{E}_g, {}^2\text{T}_{1g}\}$ levels. The spectra of the $(\text{Me}_3[9]\text{aneN}_3)\text{Mo}^{\text{III}}\text{X}_3$ complexes are similar to those of octahedral MoCl_6^{3-} ,^{7,27} even though the $(\text{Me}_3[9]\text{aneN}_3)$ complexes have lower symmetry (approximately C_{3v}). Thus, we have based the assignments on the previous work with MoCl_6^{3-} . The two spin-forbidden $d-d$ bands (${}^4\text{A}_{2g} \rightarrow {}^2\text{T}_{2g}$ and ${}^4\text{A}_{2g} \rightarrow {}^2\text{E}_g, {}^2\text{T}_{1g}$) remain almost the same in energy, whereas the two spin-allowed $d-d$ bands, ${}^4\text{A}_{2g} \rightarrow {}^4\text{T}_{2g}$ and ${}^4\text{A}_{2g} \rightarrow {}^4\text{T}_{1g}$, increase in energy in the order $\text{MoCl}_6^{3-} < (\text{Me}_3[9]\text{aneN}_3)\text{MoI}_3 < (\text{Me}_3[9]\text{aneN}_3)\text{MoBr}_3 < (\text{Me}_3[9]\text{aneN}_3)\text{MoCl}_3$. This trend is consistent with the high σ -donor strength of the triazacyclonane ligand.³⁶ Fitting the energies of the ${}^4\text{A}_{2g} \rightarrow {}^4\text{T}_{2g}$ and ${}^4\text{A}_{2g} \rightarrow {}^4\text{T}_{1g}$ transitions to a d^3 Tanabe-Sugano diagram³⁷ yields the following crystal-field parameters: $(\text{Me}_3[9]\text{aneN}_3)\text{MoCl}_3$, $Dq = 2350 \text{ cm}^{-1}$ and $B = 386 \text{ cm}^{-1}$; and $(\text{Me}_3[9]\text{aneN}_3)\text{MoBr}_3$, $Dq = 2260 \text{ cm}^{-1}$ and $B = 361 \text{ cm}^{-1}$. Brorson et al. recently performed a similar analysis on molybdenum(III) ammine

(35) Tanabe, Y.; Sugano, S. *J. Phys. Soc. Jpn.* **1954**, *9*, 766-779.

(36) See, for example: (a) Yang, R.; Zompa, L. *J. Inorg. Chem.* **1976**, *15*, 1499-1502. Wiegardt, K.; Schmidt, W.; Herrmann, W.; Küppers, H.-J. *Inorg. Chem.* **1983**, *22*, 2953-2956.

(37) Figgis, B. N. *Introduction to Ligand Fields*; Interscience: New York, 1966; p 169.

complexes, obtaining $Dq = 2465 \text{ cm}^{-1}$ and $B = 408 \text{ cm}^{-1}$ for *fac*- $\text{MoCl}_3(\text{NH}_3)_3$, as compared with $Dq = 1915 \text{ cm}^{-1}$ and $B = 433 \text{ cm}^{-1}$ for MoCl_6^{3-} .³⁸

Enemark and co-workers recently reported electronic absorption spectra for $\text{LMo}^{\text{III}}\text{X}_3$ (L = tris(3,5-dimethylpyrazolyl)-methane; X = Cl, Br, I).¹⁰ They observed weak bands in the 710–770 nm region ($\epsilon = 7\text{--}80 \text{ M}^{-1} \text{ cm}^{-1}$) in all three complexes. Because of their similarity to those outlined above for the $\text{Me}_3[9]\text{aneN}_3$ complexes, these weak bands are likely attributable to the ${}^4\text{A}_{2g} \rightarrow {}^2\text{T}_{2g}$ transition.

Flint and Paulusz's spectroscopic study of MoCl_6^{3-} showed that the Γ_7 and Γ_8 spin-orbit levels of ${}^2\text{T}_{2g}$ are separated by 255 cm^{-1} .^{27,39} Our spectra of $(\text{Me}_3[9]\text{aneN}_3)\text{MoCl}_3$ and $(\text{Me}_3[9]\text{aneN}_3)\text{MoBr}_3$ (Figures 1 and 2) also show splitting of the ${}^4\text{A}_{2g} \rightarrow {}^2\text{T}_{2g}$ band, with separations of ca. 260 and 210 cm^{-1} , respectively. This separation may reflect spin-orbit splitting of ${}^4\text{A}_{2g} \rightarrow {}^2\text{T}_{2g}$ in the $\text{Me}_3[9]\text{aneN}_3$ complexes, because of the close similarity of their spectra to that of MoCl_6^{3-} . Splitting of the ${}^4\text{A}_{2g} \rightarrow {}^2\text{T}_{2g}$ band is less obvious for $(\text{Me}_3[9]\text{aneN}_3)\text{MoI}_3$ (Figure 3).⁴⁰

We assign the luminescences of the $(\text{Me}_3[9]\text{aneN}_3)\text{MoX}_3$ complexes (see Table 2 and Figures 1–3) to phosphorescence from the lowest energy excited state ($\{{}^2\text{E}_g, {}^2\text{T}_{1g}\} \rightarrow {}^4\text{A}_{2g}$), because they show very small Stokes shifts compared to the lowest energy absorption maxima (${}^4\text{A}_{2g} \rightarrow \{{}^2\text{E}_g, {}^2\text{T}_{1g}\}$), and because their lifetimes are relatively long. The presence of increasingly heavy atoms in a molecule ordinarily increases phosphorescence decay rates and makes spin-forbidden transitions more intense. Both of these trends are observed in the $(\text{Me}_3[9]\text{aneN}_3)\text{MoX}_3$ series. The emission quantum yields are all well below 10^{-3} ; similar values have been observed in isoelectronic Cr(III) complexes.⁴¹ Radiative rate constants also increase in the order $\text{Cl} < \text{Br} < \text{I}$, as expected (estimates from lifetime and quantum yield data: ca. 60, 120, and 300 s^{-1} , respectively).

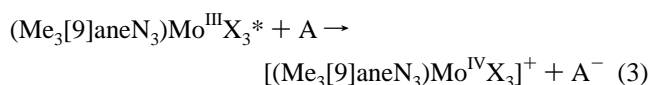
Pulsed-laser irradiation of the $(\text{Me}_3[9]\text{aneN}_3)\text{MoX}_3$ complexes produces transient absorption signals, illustrated in Figure 4, which we assign to excited-state LMCT transitions. The lowest-energy transient absorptions are red-shifted relative to the LMCT bands in the ground-state absorption spectra. The amount of the red shift, ca. 9000 cm^{-1} in each case, is approximately equal to the energy of the phosphorescent excited state. (This energy relationship is expected to hold only when the upper levels for the ground- and excited-state LMCT transitions are the same. That is not strictly true here, since the upper levels have different spin multiplicities. Thus, the lowest-lying LMCT excited states reached by absorption from ${}^4\text{A}_{2g}$ and transient absorption from $\{{}^2\text{E}_g, {}^2\text{T}_{1g}\}$ appear to be close in energy.)

Especially for $(\text{Me}_3[9]\text{aneN}_3)\text{MoCl}_3$, we found that the emission lifetime decreases somewhat as the complex concentration is increased beyond ca. 1 mM. We observed no deviation from exponential decay, even at high concentrations; therefore, we attribute the quenching to reaction with the ground state of the complex.⁴²

$\text{HB}(\text{Me}_2\text{pz})_3\text{MoCl}_3^-$ and *mer*- $\text{MoCl}_3(\text{py})_3$ phosphoresce more weakly and at longer wavelengths than the $\text{Me}_3[9]\text{aneN}_3$ complexes. In the case of *mer*- $\text{MoCl}_3(\text{py})_3$ the red shift may be due in part to the lower-symmetry (C_{2v}) meridional coordination environment.

We could not undertake a detailed photophysical and photochemical study of $(\text{Me}_3[9]\text{aneN}_3)\text{W}^{\text{III}}\text{Cl}_3$ because of the difficulty in purifying the complex. However, as indicated by both the electronic absorption and emission spectra discussed above, there are close similarities between $(\text{Me}_3[9]\text{aneN}_3)\text{W}^{\text{III}}\text{Cl}_3$ and other third-row d^3 ions.

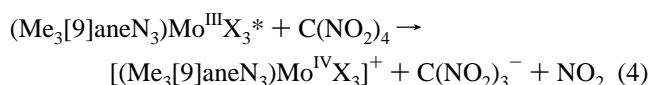
Reversible Photooxidation. The phosphorescence quenching that we observe in the presence of electron acceptors (A) is consistent with reversible one-electron transfer:



Since the lowest triplet states of the electron acceptors⁴³ are higher in energy than the phosphorescent $\{{}^2\text{E}_g, {}^2\text{T}_{1g}\}$ excited states of the metal complexes, energy transfer quenching is very unlikely. TCNE, the most powerfully oxidizing quencher we studied, shows the largest quenching rate constants; BV^{2+} , the weakest oxidant, reacts much more slowly.

A more detailed study of reversible photooxidation of these complexes might help to determine whether their excited states, which are ligand-field in character, differ in their properties (e.g. reorganizational energy) from those of MLCT states (e.g. $\text{Ru}(\text{bpy})_3^{2+}$) or other types of metal-complex excited states. However, this has not been possible: mainly because of the low energy of the $(\text{Me}_3[9]\text{aneN}_3)\text{Mo}^{\text{III}}\text{X}_3$ excited states, they are poorer reducing agents (see data in Table 2) than species such as $\text{Ru}(\text{bpy})_3^{2+*}$. As a result, suitable oxidative quenchers for $\text{Mo}(\text{III})^*$ must be relatively powerful oxidizing agents. Only a very small number of compounds are available that have sufficiently positive electrode potentials for reduction⁴⁴ and do not interfere spectroscopically with excitation of the $\text{Mo}(\text{III})$ complexes.

Irreversible Photooxidation. We observe permanent one-electron photooxidation of $(\text{Me}_3[9]\text{aneN}_3)\text{Mo}^{\text{III}}\text{Br}_3$ and $(\text{Me}_3[9]\text{aneN}_3)\text{Mo}^{\text{III}}\text{I}_3$ by $\text{C}(\text{NO}_2)_4$, leading to the formation of $[(\text{Me}_3[9]\text{aneN}_3)\text{Mo}^{\text{IV}}\text{X}_3]^+$:



We also performed this photooxidation in the presence of water, to determine whether reaction 4 could be followed by further oxidation to Mo^{V} , either by disproportionation (eq 5) or by reaction with additional $\text{C}(\text{NO}_2)_4$ (eq 6):

(38) Brorson, M.; Jacobsen, C. J. H.; Jensen, C. M.; Schmidt, I.; Villadsen, J. *Inorg. Chim. Acta* **1996**, *247*, 189–194.

(39) The room-temperature absorption spectrum of MoCl_6^{3-} in concd HCl (aq) shows a less well-defined splitting of the ${}^4\text{A}_{2g} \rightarrow {}^2\text{T}_{2g}$ transition, with a separation of ca. 200 cm^{-1} .

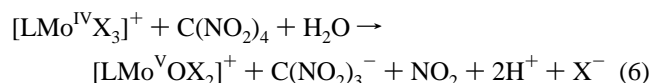
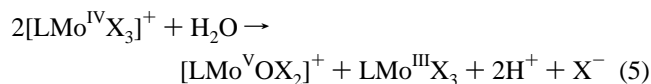
(40) More detailed examination of the ${}^4\text{A}_{2g} \rightarrow {}^2\text{T}_{2g}$ band in $(\text{Me}_3[9]\text{aneN}_3)\text{Mo}^{\text{III}}\text{I}_3$ suggests that it may be composite, being made up of bands at ca. 710 and 722 nm (i.e. separated by ca. 230 cm^{-1}). Also, this band is slightly wider in $(\text{Me}_3[9]\text{aneN}_3)\text{Mo}^{\text{III}}\text{I}_3$ (fwhm 41 nm) than in the chloride (29 nm) and bromide (33 nm) complexes.

(41) See, for example: Kirk, A. D.; Porter, G. B. *J. Phys. Chem.* **1980**, *84*, 887–891.

(42) Other authors have also studied ground-state quenching in d^3 complexes. See, for example: Serpone, N.; Jamieson, M. A.; Sriram, R.; Hoffman, M. Z. *Inorg. Chem.* **1981**, *20*, 3983–3988.

(43) The energy for the lowest triplet state for chloranil, for example, is 2.13 eV: Guerry-Butty, E.; Haselbach, E.; Pasquier, C.; Suppan, P.; Phillips, D. *Helv. Chim. Acta* **1985**, *68*, 912–918. Since the other acceptors are colorless, they are also expected to have higher-lying triplet excited states.

(44) The quenchers studied here include most of the strongest oxidants listed in the following: Mann, C. K.; Barnes, K. K. *Electrochemical Reactions in Nonaqueous Solvents*; Dekker: New York, 1970.



Reaction 5 is similar to our previous work with $\text{Mo}^{\text{III}}(\text{NCS})_6^{3-}$, in which one-electron photooxidation to $\text{Mo}^{\text{IV}}(\text{NCS})_6^{2-}$ was followed by disproportionation to generate the molybdenum(V) dimer $\text{Mo}_2^{\text{V}}\text{O}_4(\text{NCS})_6^{4-}$.⁵ An analog of reaction 6 is the photoinitiated two-electron oxidation of $\text{V}(\text{phen})_3^{2+}$ to VO^{2+} ; this proceeds via a vanadium(III) intermediate, which is oxidized spontaneously by a second molecule of electron acceptor.⁴

Samples of $[(\text{Me}_3[9]\text{aneN}_3)\text{Mo}^{\text{IV}}\text{Br}_3]^+$, prepared separately, are stable in pure CH_3CN but disproportionate in $\text{CH}_3\text{CN}-\text{H}_2\text{O}$ mixtures, forming $(\text{Me}_3[9]\text{aneN}_3)\text{Mo}^{\text{III}}\text{Br}_3$ and $[(\text{Me}_3[9]\text{aneN}_3)\text{Mo}^{\text{V}}\text{OBr}_2]^+$. These disproportionation products were identified by visible (sharp maximum near 690 nm for Mo(III), and broad band centered at 670 nm for Mo(V)) and IR spectroscopy (ν_{MoO} for Mo(V)).⁸ Also, our cyclic voltammetry data for the oxidation of $(\text{Me}_3[9]\text{aneN}_3)\text{Mo}^{\text{III}}\text{Br}_3$ and $(\text{Me}_3[9]\text{aneN}_3)\text{Mo}^{\text{III}}\text{I}_3$ in aqueous mixtures (see Table 4) show that the Mo(III)/Mo(IV) wave becomes less reversible as more H_2O is added. This is also consistent with disproportionation of $[(\text{Me}_3[9]\text{aneN}_3)\text{Mo}^{\text{IV}}\text{X}_3]^+$ in the presence of water. In contrast, $[(\text{Me}_3[9]\text{aneN}_3)\text{Mo}^{\text{IV}}\text{Br}_3]^+$ in CH_3CN does not react with $\text{C}(\text{NO}_2)_4$.

Photooxidation of $(\text{Me}_3[9]\text{aneN}_3)\text{Mo}^{\text{III}}\text{Br}_3$ by $\text{C}(\text{NO}_2)_4$ in 1:1 $\text{CH}_3\text{CN}-\text{H}_2\text{O}$ yields $[(\text{Me}_3[9]\text{aneN}_3)\text{Mo}^{\text{V}}\text{OBr}_2]^+$ as the only Mo-containing product. Thus, $(\text{Me}_3[9]\text{aneN}_3)\text{Mo}^{\text{III}}\text{Br}_3$ undergoes photoinitiated two-electron oxidation. Our experiments described above using Mo(IV) indicate that this occurs via initial one-electron photooxidation of Mo(III) (reaction 4), followed by disproportionation of $[(\text{Me}_3[9]\text{aneN}_3)\text{Mo}^{\text{IV}}\text{Br}_3]^+$, as in reaction 5.

Reactions 5 and 6 differ only in the nature of the oxidizing agent: $[(\text{Me}_3[9]\text{aneN}_3)\text{Mo}^{\text{IV}}\text{Br}_3]^+$ in eq 5, and $\text{C}(\text{NO}_2)_4$ in eq 6. $(\text{Me}_3[9]\text{aneN}_3)\text{Mo}^{\text{III}}\text{Br}_3$ is already known not to react spontaneously with $\text{C}(\text{NO}_2)_4$; this suggests that the Mo^{IV} complex is the stronger of the two oxidants.⁴⁵ Therefore, the disproportionation route is consistent with our other chemical observations.

$(\text{Me}_3[9]\text{aneN}_3)\text{MoI}_3$ is also photooxidized to the Mo^{V} complex $[(\text{Me}_3[9]\text{aneN}_3)\text{MoOI}_2]^+$ by $\text{C}(\text{NO}_2)_4$ in the presence of water.

(45) This conclusion must be reached cautiously, since the reduction of $\text{C}(\text{NO}_2)_4$ (which we observe at ca. -0.5 V vs Fc/Fc^+ in CH_3CN) is irreversible.

This system was more difficult to study for two reasons. First, we were unable to prepare the proposed Mo^{IV} intermediate, $[(\text{Me}_3[9]\text{aneN}_3)\text{Mo}^{\text{IV}}\text{I}_3]^+$, in stable form so that its reactivity with H_2O and $\text{C}(\text{NO}_2)_4$ could be compared. Second, the photooxidation of Mo^{III} to Mo^{V} is not as complete as with the bromide complex. However, the discussion of $(\text{Me}_3[9]\text{aneN}_3)\text{Mo}^{\text{III}}\text{Br}_3$ above is equally applicable here: $[(\text{Me}_3[9]\text{aneN}_3)\text{Mo}^{\text{IV}}\text{I}_3]^+$ is a slightly stronger oxidant than the corresponding bromomolybdenum(IV) complex, making it also unlikely that $(\text{Me}_3[9]\text{aneN}_3)\text{MoI}_3$ could be oxidized spontaneously by $\text{C}(\text{NO}_2)_4$. Thus, the photoinitiated two-electron oxidation in the $(\text{Me}_3[9]\text{aneN}_3)\text{MoI}_3$ and $(\text{Me}_3[9]\text{aneN}_3)\text{MoBr}_3$ systems are likely to occur by the same mechanism.

Summary

The three $(\text{Me}_3[9]\text{aneN}_3)\text{Mo}^{\text{III}}\text{X}_3$ complexes ($\text{X} = \text{Cl}, \text{Br}, \text{I}$) phosphoresce in solution at room temperature, and their excited states are oxidized reversibly by several one-electron acceptors. Permanent one-electron photooxidation of $(\text{Me}_3[9]\text{aneN}_3)\text{Mo}^{\text{III}}\text{Br}_3$ and $(\text{Me}_3[9]\text{aneN}_3)\text{Mo}^{\text{III}}\text{I}_3$ occurs in the presence of $\text{C}(\text{NO}_2)_4$. Overall two-electron oxidation of the same two complexes occurs via disproportionation of photogenerated Mo^{IV} intermediates in the presence of water. $[\text{HB}(\text{Me}_2\text{pz})_3\text{Mo}^{\text{III}}\text{Cl}_3]^-$, $\text{MoCl}_3(\text{py})_3$, and $(\text{Me}_3[9]\text{aneN}_3)\text{W}^{\text{III}}\text{Cl}_3$ also phosphoresce at room temperature. The properties of the $\text{Me}_3[9]\text{aneN}_3$ species in particular suggest that a variety of stable d^3 complexes are accessible for multielectron photoredox experiments and that many of them are likely to undergo facile photoinitiated two-electron oxidation. We are now studying the chemistry and photochemistry of the higher oxidation states in these and related Mo systems,⁴⁶ including their reactivity with oxidizable substrate molecules.⁴⁷

Acknowledgment. We are grateful to Professors Russell H. Schmehl, Erwin D. Poliakoff, and Paul R. Sharp for experimental assistance. This research was supported by grants from the National Science Foundation and the Louisiana Educational Quality Support Fund (administered by the Louisiana Board of Regents). Some of the experiments and data analyses were performed at the Center for Fast Kinetics Research, supported jointly by the Biomedical Research Technology Program of the Division of Research Resources of the National Institutes of Health and by The University of Texas at Austin.

IC970955R

(46) Mohammed, A. K.; Maverick, A. W. *Inorg. Chem.* **1992**, *31*, 4441–4443.

(47) Isovitsch, R. A.; Fronczek, F. R.; Maverick, A. W. Submitted for publication.